Chalcogenide Letters Vol. 15, No. 8, August 2018, p. 411 - 417

EFFECT OF $GeSe_2$ ON THE PREPARATION AND PROPERTIES OF $Cu_2Zn(Sn,Ge)(S,Se)_4$ FILMS

C. GAO[a*], L. DU[b], X TENG[b], W. YU[b]
[a]*Institute of Photovoltaics, Nanchang University, Nanchang 330031, China*
[b]*College of Physics Science and Technology, Hebei University, Baoding 071002, China*

In this paper, $Cu_2Zn(S,Ge)(S,Se)_4$ (CZTGSSe) films were prepared by selenizing sputtered Cu-Zn-Sn-S precursor films with Se and $GeSe_2$. For comparison, normal $Cu_2ZnSn(S,Se)_4$ (CZTSSe) films were prepared by selenizing the same precursor films with only Se. By comparing the properties of CZTSSe and CZTGSSe films, the effect of $GeSe_2$ on the preparation and properties of CZTGSSe films was investigated. For CZTSSe films, we noticed that the CZTSSe material tend to decompose especially after a long selenization process. The decomposition of the material will result in the Sn-loss and the porous morphology of the film. When $GeSe_2$ was added during the selenization process, Ge can be incorporated into the film, which will compensate the loss of Sn and prevent the decomposition of the material. Moreover, the Ge-incorporation can promote the crystal growth and modify the defect formation in the material. Based on CZTGSSe material, solar cells with efficiencies up to 6.5% have been prepared.

(Received April 12, 2018; Accepted August 7, 2018)

Keywords: $Cu_2Zn(S,Ge)(S,Se)_4$, Selenization, $GeSe_2$, Solar cell

1. Introduction

$Cu_2ZnSn(S,Se)_4$ (CZTSSe) is a promising photovoltaic material. This material has the advantages such as suitable optical band-gap, high absorption coefficient and earth-abundant constituted elements [1,2]. CZTSSe material and solar cells have attracted the attentions of photovoltaic researchers during the last years. Currently, the best CZTSSe solar cell have reached the efficiency of 12.6% [3].

CZTSSe material can be prepared by many methods including co-evaporation [4], sputtering [5], spin-coating [6], etc. Among these methods, sputtering is a mature method that widely used in industry. If a uniform compound target is used for sputtering, the preparation of a large and uniform film could be feasible. So, sputtering would be promising in preparing high quality CZTSSe films.

To improve the efficiency of CZTSSe solar cell, the properties of CZTSSe material should be optimized. About the CZTSSe material, currently the quality of the material is normally lower than the quality of the commercial photovoltaic material such as $Cu(In,Ga)Se_2$. This is probably related with the complex formation mechanism of intrinsic defects, the formation of secondary phases in this material, etc [2]. By alloying with Ge (i.e., $Cu_2Zn(Sn,Ge)(S,Se)_4$), people found the deep level defects or the band-tail related defects in the material could be partly eliminated [7-9]. Moreover, Ge is believed can form specific liquid phase with Se during the selenization process, which is beneficial to the crystallization of the material. Therefore, by alloying with Ge, high quality $Cu_2Zn(Sn,Ge)(S,Se)_4$ (CZTGSSe) material with less un-favorable defects and good crystallinity could be prepared.

In this paper, we prepared CZTGSSe material by using sputtering and a novel selenization process. For this method, Cu-Zn-Sn-S precursor films were firstly prepared by sputtering a compound target, then the precursor films were selenized in a graphite box with Se pellets and $GeSe_2$ powder. For comparison, CZTSSe films without Ge-alloying were prepared by selenizing the Cu-Zn-Sn-S precursor films with only Se pellets. The influence of $GeSe_2$ on the morphology,

* Corresponding author: cgao@ncu.edu.cn

composition and crystallinity of the prepared films were investigated. Based on the CZTSSe and CZTGSSe films, solar cells were fabricated and compared.

2. Experiments

2.1. Preparation of material and solar cell

For the preparation of CZTSSe and CZTGSSe films, Mo-coated soda lime glass were used as substrates. After the cleaning of the substrates, Cu-Zn-Sn-S precursor films were deposited on the substrates by sputtering a $Cu_{1.8}Zn_{1.1}Sn_{0.9}S_3$ compound target. For the sputtering, the pressure of the Ar gas and the sputtering power were 0.3Pa and 70W, respectively. After 2h of sputtering, precursor films with the thicknesses of around 1 μm were obtained.

After the preparation of the precursor films, they were put into a graphite box which contained Se pellets and $GeSe_2$ powder for CZTGSSe material, or only Se pellets for CZTSSe material. The Se pellets and $GeSe_2$ powder were placed in small ceramic crucibles, which were separated from the precursor film. For the selenization process, the graphite box was firstly transferred into a tube furnace. Then the tube was evacuated and refilled with nitrogen to the pressure of 100 Torr. After that the temperature of the furnace was ramped up to 600℃ and maintained for 15 or 30 min for different preparation. Finally, the furnace was naturally cooled down to room temperature. Here the CZTGSSe films selenized for 15min and 30min were named as Ge15 and Ge30, respectively. The CZTSSe films selenized for 15min and 30min were named as Se15 and Se30, respectively.

By using CZTSSe and CZTGSSe films as absorber layers, solar cells were fabricated with the structure of Mo/CZT(Ge)SSe/CdS/i-ZnO/AZO/Ag. In this structure, Mo layer with the thickness of 1μm was prepared by sputtering. CdS layer of around 50 nm was prepared by chemical bath deposition. I-ZnO and AZO layers were deposited by sputtering. Ag grid with the thickness of around 200 nm was prepared by thermal evaporation.

2.2. Characterizations

The morphologies and compositions of the films were measured by a JSM-7500F scanning electron microscopy (SEM) equipped with energy dispersive X-ray spectroscopy (EDS). The constitutions of the films are analyzed using a Bruker D8 Advance X-ray diffractometer. The Raman spectra of the films were recorded by a JY LabRAM HR Evolution Raman spectrometer with the excitation laser of 532 nm. I-V curves of the solar cells were measured under AM 1.5G illumination using an Agilent B1500A semiconductor parameter analyzer.

3. Results and discussions

Fig. 1 shows the XRD patterns of the films selenized with Se or Se+$GeSe_2$. The diffraction peaks at around 40° and 44° are caused by the Mo back contact and the sample holder for the XRD measurement.

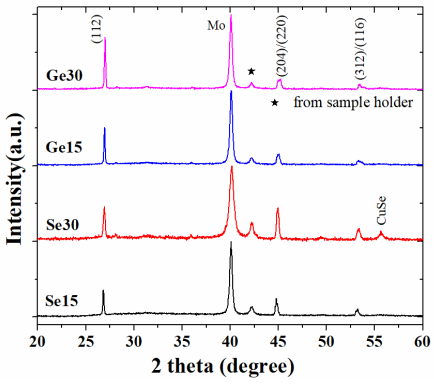

Fig.1. XRD patterns of the films selenized with Se and Se+$GeSe_2$

All the XRD patterns show three main diffraction peaks at around 27°, 45° and 53°, which can be attributed to the (112), (220), and (312) reflexes of kesterite structure [9]. For Se30 sample, an additional diffraction peak can be seen at around 56°, which can be attributed to CuSe (JCPDS 89-2734). Except that, no obvious secondary phase is indicated for all the other samples. Therefore, for Se15 and Se30 samples, the main phase in the films should be CZTSSe. As the selenization time increases, CuSe secondary phase is formed in the film. For Ge15 and Ge30 samples, since Ge is incorporated (Table 1) but no Ge-related secondary phase is detected, the main phase in these films should be CZTGSSe. As the selenization time increases, no obvious secondary phase is formed in CZTGSSe films.

Fig.2 shows the SEM images of the films by different preparations. By comparing the SEM images, it is found the grain sizes in the films can be greatly increased by using $GeSe_2$ during selenization. EDS results prove that Ge is incorporated into the films that selenized with $GeSe_2$ (Ge/(Ge+Sn) is 0.39 and 0.46 for the films selenized for 15 min and 30 min, respectively). Since the precursor films contain no Ge, as well as the $GeSe_2$ powder don't directly contact with the precursor films during the selenization, the mechanism of the Ge-incorporation for the films selenized with $GeSe_2$ is a little complex. We believe the solid $GeSe_2$ can partly vaporize during the high-temperature selenization process. The $GeSe_2$ vapor can contact the precursor films and make Ge incorporated into the films. As discussed in reference, the incorporated Ge may react with Se to form specific liquid phase. So, the diffusion of the elements may be promoted during the selenization, which may be the reason for the increased grain sizes in the films.

As the selenization time increases, the grain sizes in both the CZTSSe and CZTGSSe films do not increase significantly. For CZTGSSe films, both the Ge15 and Ge30 films show compact morphologies. However, for CZTSSe films, the morphology of the film becomes porous when the selenization time increases from 15 min to 30 min. The compositions of the films before and after selenization are analyzed by EDS and the results are shown in Table 1. The composition of the precursor film is Cu/(Zn+Sn)=0.81 and Zn/Sn=1.19, which is close to the composition of the sputtering target. After the normal selenization, the Zn/Sn ratio of the films increases significantly (1.50 for the Se15 film and 1.66 for the Se30 film). At high temperature (>500℃), the following equilibrium reaction exist for the CZTSSe material [10]:

$Cu_2ZnSn(S,Se)_4 \leftrightarrow Cu_x(S,Se)+Zn(S,Se)+Sn(S,Se)+(S,Se)_2$

Since Sn(S,Se) is volatile at high temperature, the equilibrium reaction tend to shift to the right side. Therefore, a long annealing process can decompose the CZTSSe material and result in the loss of Sn. Here, the increased Zn/Sn ratios and the formation of CuSe secondary phase in Se30 film should result from the decomposition of CZTSSe material. As the decomposition of CZTSSe material, the film may show the porous morphology (Fig.2(b) for Se30 sample).

By contrast to the CZTSSe films, the Zn/(Ge+Sn) ratio of the CZTGSSe films increase slightly after the selenization (1.14 for the Ge15 sample and 1.22 for the Ge30 sample). EDS results reveal that Ge content is increased as the selenization time increases. For CZTGSSe films, the equilibrium reaction at high temperature should be:

$$Cu_2Zn(Sn,Ge)(S,Se)_4 \leftrightarrow Cu_x(S,Se)+Zn(S,Se)+Sn(S,Se)+(S,Se)_2+GeSe_2$$

Since Sn(S,Se) is volatile and no additional Sn(S,Se) is available at the surface of the material. The reaction will shift to the right side. So the CZTGSSe material will decompose which result in the loss of Sn. However, when $GeSe_2$ vapor exist at the surface of the material, the $GeSe_2$ may react with the decomposed $Cu_x(S,Se)$ and Zn(S,Se), and shift the following equilibrium reaction to the left side:

$$Cu_2ZnGe(S,Se)_4 \leftrightarrow Cu_x(S,Se)+Zn(S,Se)+(S,Se)_2+GeSe_2$$

Therefore, the decomposition of the material and the formation of secondary phases could be prevented when $GeSe_2$ vapor exist during the selenization. The incorporated Ge will diffuse from the surface into the bulk of the material then (actually, XPS measurement reveal that Ge exists at the back side of the material).

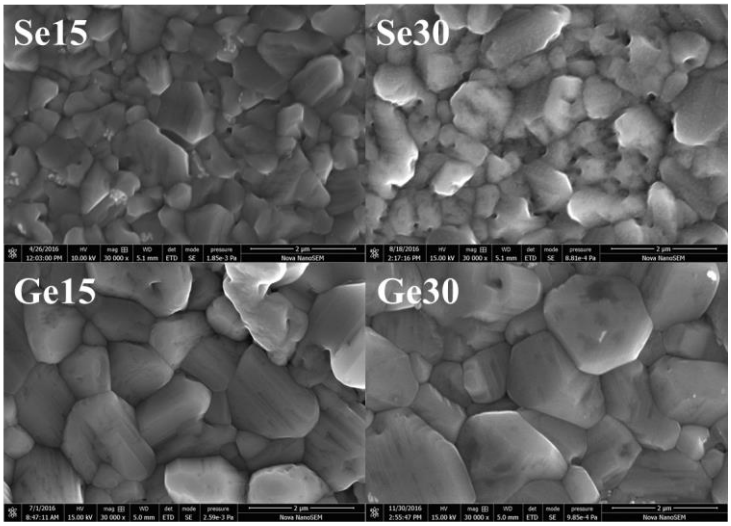

Fig. 2 SEM images of CZTSSe / CZTGSSe thin films prepared at different selenization time

Table 1. Compositions of the precursor and selenized films

Sample	Cu/(Zn+Sn)	Zn/(Sn+Ge)	Ge/(Sn+Ge)
precursor	0.81	1.19	-
Se15	0.83	1.50	-
Se30	0.86	1.66	-
Ge15	0.79	1.14	0.31
Ge30	0.82	1.22	0.46

Fig. 3 shows the Raman spectra of the films. All the Raman spectra of the films show two main Raman peaks at around 175 cm^{-1} and 200 cm^{-1}, which is close to the Raman mode of $Cu_2ZnSnSe_4$ [11]. The weak and broad peaks at around 240cm^{-1} could be related with the secondary phases such as ZnSe, CuSe or $MoSe_2$ [12]. Compare to the Raman spectra of the CZTSSe films, the Raman spectra of the CZTGSSe films are flatter at the region around 240cm^{-1}, indicating that the CZTGSSe films may contain less secondary phases.

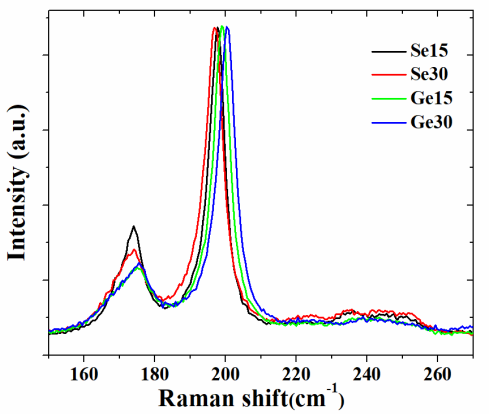

Fig. 3. Raman spectra of the CZTSSe and CZTGSSe thin films

From the Raman spectra we can clearly see the shift of the main Raman peak between different samples. Actually, the position of the (112) diffraction peak in the XRD patterns also shifts between the samples. The shift of the XRD and Raman peaks of different samples are shown in Fig. 4. For CZTSSe films, as the selenization time increases, the (112) diffraction peak and the main Raman peak shift to low angle and high wavenumber, respectively. This could be caused by the decomposition of the CZTSSe material. When $GeSe_2$ is introduced for the selenization, the (112) diffraction peak and the main Raman peak shift to high angle and high wavenumber, respectively. The reason for this could be that the Ge-incorporation shrinks the lattice parameters and modifies the vibration mode of the material. Except for the position of the XRD and Raman peaks, we also record the FWTH (full width at half maxima) of the (112) diffraction peak and the main Raman peak for different samples. For CZTSSe samples, both the XRD and Raman peaks broaden significantly as the selenization time increases, indicating the decreased crystallinity of material (could be caused by the decomposition of the material). For CZTGSSe films, as the selenization time increases, the FWTH of the XRD and Raman peaks increases slightly. Since no obvious secondary phase are detected in Ge30 sample, as well as the composition of Ge30 sample don't show obvious different compare to Ge15 sample. The broaden of the XRD and Raman peaks may not be caused by the decomposition of the material. In reference [13], the authors suggested the broaden of the diffraction peak for Ge-alloy CZTSSe films could be caused by the non-uniform distribution of the Ge element in the material (i.e., some of the region may be Ge-rich but other regions may be Ge-poor in composition). As Ge is diffused from the surface to the bulk of the material, we believe the distribution of Ge is not homogeneous in our samples.

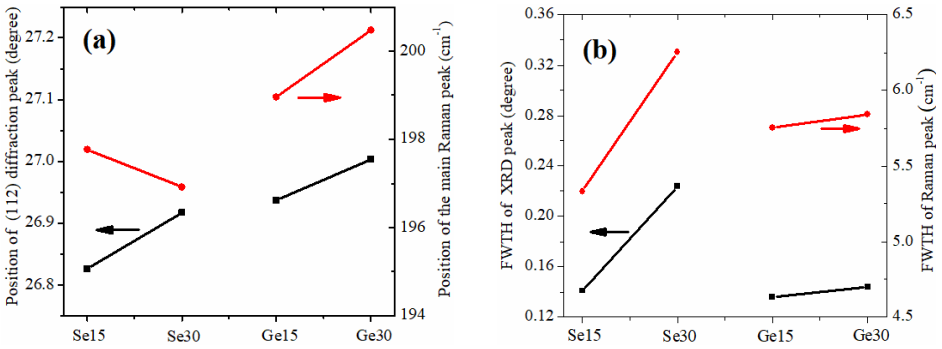

Fig. 4. Position and FWTH of the (112) diffraction peak and the main Raman peak

Besides, we found the relative intensity of the Raman peak at 175 cm^{-1} is decreased by the Ge-incorporation. According to reference, the changes of the relative intensities of the Raman peaks could be related with the population of intrinsic defects or defect clusters in the material [14]. The decrease of the relative intensity for the 175 cm^{-1} peak indicates the increase of the concentration of $[V_{Cu}+Zn_{Cu}]$ defect cluster in the material, which is believed beneficial to the material quality. Therefore, the formation of the intrinsic defects in the material can be modified by the Ge-incorporation.

Based on the CZTSSe and CZTGSSe films, solar cells were fabricated. The I-V curves and the key performance parameters of the solar cells are shown in Fig.5 and Table 2, respectively. The solar cell based on Se15 achieves the efficiency of 3.7%. Compare to that, solar cell based on Se30 shows significantly decreased efficiency (1.0%). This could be caused by that the long selenization process decomposed the material and deteriorated the electrical properties of the absorber layer. When $GeSe_2$ was used during the selenization, the fill factor of the solar cell increases obviously. Therefore, even the open circuit voltage and short-circuit current density of the solar cell based on Ge15 is lower than that of the solar cell based on Se15, the efficiency of the solar cell increases from 3.6% to 5.0%. The solar cell based on Ge30 achieves the best efficiency of 6.5%, which indicates that the Ge-incorporation can improve the properties of the absorber layer.

As we discussed above, the $GeSe_2$ can prevent the decomposition of the material, so a relative long selenization process can be used to improve the crystallinity of the material.

Moreover, the Ge-incorporation can promote the crystal growth and modify the defect formation in the material. These could be the reasons that why the usage of $GeSe_2$ can improve the properties of the material and the solar cell.

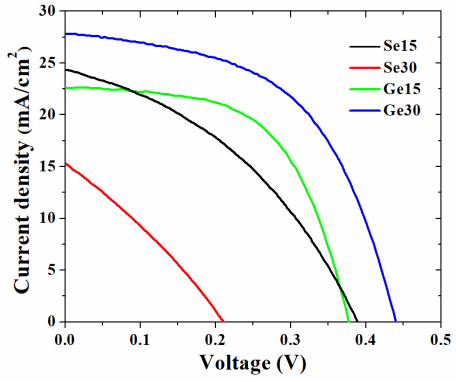

Fig. 4. I-V curves of the solar cell based on CZTSSe and CZTGSSe layers

Table 2. The performance parameters of the CZTSSe and CZTGSSe solar cells

	V_{oc} (mV)	J_{sc} (mA/cm^2)	Fill factor (%)	Efficiency (%)
Se15	389	24.3	39.2	3.7
Se30	210	15.1	30.0	1.0
Ge15	377	22.6	58.9	5.0
Ge30	440	27.8	53.5	6.5

4. Conclusions

CZTGSSe films were prepared by selenizing sputtered Cu-Zn-Sn-S precursor films with Se and $GeSe_2$ in the graphite box. For comparison, CZTSSe films were prepared by selenizing the precursor films with only Se. The effect of $GeSe_2$ on the properties of the films were investigated by comparing the properties of CZTSSe and CZTGSSe films. We believe the solid $GeSe_2$ should vaporize due to the high temperature of the selenization process.

The existence of $GeSe_2$ vapor around the precursor films will incorporate Ge in the films (compensate the loss of Sn during the selenization) and prevent the decomposition of the material. Furthermore, when $GeSe_2$ was used for the selenization, the growth of the crystalline grains was obviously promoted. The incorporation of Ge may also modify the defect formation of the material, making the films more suitable for the solar cells fabrication. Base on CZTGSSe layers, solar cells with efficiencies up to 6.5% were prepared.

Acknowledgements

This work has been supported by the National Natural Science Foundation of China (Grant No. 61504054) and the Natural Science Foundation of Jiangxi Province (Grant No. 20171BAB212018).

References

[1] X. Liu, Y. Feng, H. Cui, F. Liu, X. Hao, G. Conibeer, D.B. Mitzi, M. Green, Prog. Photovoltaics Res. Appl. **24**, 879 (2016).
[2] A. Polizzotti, I.L. Repins, R. Noufi, S.-H. Wei, D.B. Mitzi, Energy Environ. Sci. **6**, 3171 (2013).
[3] W. Wang, M.T. Winkler, O. Gunawan, T. Gokmen, T.K. Todorov, Y. Zhu, D.B. Mitzi, Adv. Energy Mater. **4**, 1301465 (2014).
[4] Y. S. Lee, T. Gershon, O. Gunawan, T. K. Todorov, T. Gokmen, Y. Virgus, S. Guha, Adv. Energy Mater. **5,** 1401372 (2015).
[5] R. Bodeux, F. Mollica, S. Delbos, Sol. Energy Mater. Sol. Cells. **132**, 67 (2015).
[6] S. G. Haass, M. Diethelm, M. Werner, B. Bissig, Y. E. Romanyuk, A. N. Tiwari, Adv. Energy Mater. **5**, 1 (2015).
[7] S. Giraldo, E. Saucedo, M. Neuschitzer, F. Oliva, M. Placidi, X. Alcobé, V. Izquierdo-Roca, S. Kim, H. Tampo, H. Shibata, A. Pérez-Rodríguez, P. Pistor, Energy Environ. Sci. **11**, 582 (2018).
[8] S. Giraldo, M. Neuschitzer, T. Thersleff, S. Loepez-Marino, Y. Saenchez, H. Xie, M. Colina, M. Placidi, P. Pistor, V. Izquierdo-Roca, K. Leifer, A. Peerez-Rodrieguez, E. Saucedo, Adv. Energy Mater. **5**, 1501070 (2015).
[9] S. Kim, K. M. Kim, H. Tampo, H. Shibata, K. Matsubara, S. Niki, Sol. Energy Mater. Sol. Cells. **144**, 488 (2016).
[10] A. Redinger, D. M. Berg, P. J. Dale, S. Siebentritt, J. Am. Chem. Soc. **133**, 3320 (2011).
[11] M. Ganchev, J. Iljina, L. Kaupmees, T. Raadik, O. Volobujeva, A. Mere, M. Altosaar, J. Raudoja, E. Mellikov, Thin Solid Films. **519**, 7394 (2011).
[12] C. Fella, A. Uhl, Y. Romanyuk, A. Tiwari, Phys. Status Solidi. **209**, 1043 (2012).
[13] J. Márquez, H. Stange, C. Hages, N. Schaefer, S. Levcenko, S. Giraldo, E. Saucedo, K. Schwarzburg, D. Abou-Ras, A. Redinger, M. Klaus, C. Genzel, T. Unold, R. Mainz, Chem. Mater. **29**, 9399 (2017).
[14] M. Dimitrievska, A. Fairbrother, E. Saucedo, A. Peerezrodrieguez, V. Izquierdoroca, Appl. Phys. Lett. **106**, 073903 (2015).